Reactivity of Ferrocenylboranes: Rearrangements versus Electron Transfer Reactions

Li Ding,[†] Fabrizia Fabrizi de Biani,[‡] Michael Bolte,[§] Piero Zanello,[‡] and Matthias Wagner*,[†]

Institut für Anorganische Chemie, J. W. Goethe-Universität Frankfurt, Marie-Curie-Strasse 11, D-60439 Frankfurt (Main), Germany, Dipartimento di Chimica dell'Università, Via Aldo Moro, I-53100 Siena, Italy, and Institut für Organische Chemie, J. W. Goethe-Universität Frankfurt, Marie-Curie-Strasse 11, D-60439 Frankfurt (Main), Germany

Received August 22, 2000

The chemical behavior of ferrocenylboranes FcB(R)R′ (Fc = $C_5H_5FeC_5H_4$) toward 2,5-bis(pyrazol-1-yl)benzoquinone (**1**) is highly dependent on the nature of the substituents R and R′. Reaction of **1** with 2 equiv of the ferrocenylborane $FcBMe_2$ (**2a**) results in an unprecedented sequence of methyl migration and elimination steps; the Fe(II) oxidation state of the Fc fragments remains unchanged. In contrast, electron-transfer processes involving iron oxidation and benzoquinone reduction dominate the reaction of **1** with FcB(Me)Br (**2b**) and $FcBBr_2$ (**2c**). Despite these different reactivities, bis(ferrocenyl) complexes with a bridging hydroquinone ligand (**3a**, [**3b**]Br_2, [**3c**]Br_2) are formed in all three cases.

Introduction

Reaction of decamethylferrocene ($FeCp^*_2$) with tetracyanoethylene (TCNE) gives the charge-transfer (CT) complex $[FeCp^*_2]^+[TCNE]^-$, which exhibits bulk ferromagnetic properties with a spontaneous magnetization below T_c = 4.8 K (**I**, Figure 1).[1,2] In this kind of substance, the degree of spin−spin coupling is highly dependent on the packing of the donor (D) and acceptor (A) components in the crystal lattice. The development of novel ferrocene-based electron donors, which allow one to influence the redox potential of the iron core and to control the relative orientation of D and A, is therefore of great current interest.

We have recently shown that the redox potential of adducts of the diborylated ferrocene 1,1′-fc$(BMe_2)_2$ (fc = $C_5H_4FeC_5H_4$) with nitrogen bases is similar to that of decamethylferrocene but can be fine-tuned by varying the basicity of the N-donor.[3] In a series of preliminary experiments, the reaction of 1,1′-fc$(BMe_2{\cdot}py)_2$ (py = pyridine) with tetracyanoquinone was investigated and shown to yield a green paramagnetic CT salt. Magnetic susceptibility measurements on this compound showed a significant deviation from the Curie−Weiss law.[4] However, single crystals of the material have not been obtained, which is therefore still only poorly characterized.

On the basis of this result, we are now suggesting a novel concept for the generation of well-defined ferrocene-containing CT salts. The system consists of (i) organic electron acceptors bearing two Lewis-basic amine substituents and (ii) derivatives of ferrocenylboranes. When both components are brought together, the formation of B−N adducts is thought to activate the ferrocene donor and at the same time to bring the organic acceptor into close proximity. The purpose of this paper is to describe experimental results proving the general validity of our concept and providing valuable information regarding the future design of more sophisticated molecular building blocks. The final goal of our ongoing research is to generate polymeric structures such as **II** (Figure 1).

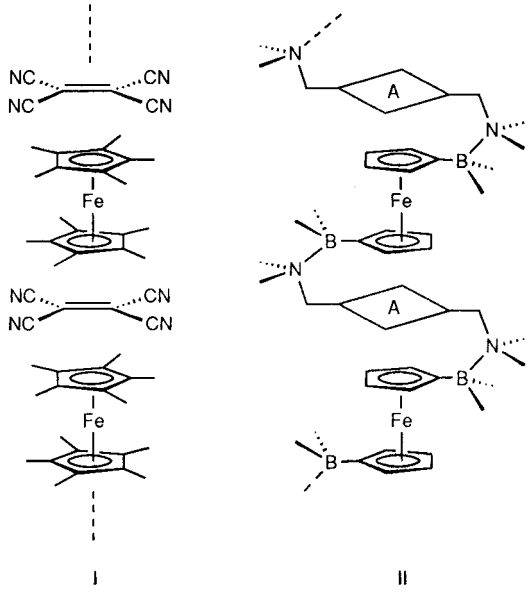

Figure 1. The organometallic compound **I** showing bulk ferromagnetism in the solid state and a schematic representation of the charge-transfer target compound **II** with a B−N backbone (A = electron acceptor).

* To whom correspondence should be addressed. Fax: +49 69 798 29260. E-mail: Matthias.Wagner@chemie.uni-frankfurt.de.
[†] Institut für Anorganische Chemie, J. W. Goethe-Universität Frankfurt.
[‡] Dipartimento di Chimica dell'Università.
[§] Institut für Organische Chemie, J. W. Goethe-Universität Frankfurt.

(1) Miller, J. S.; Calabrese, J. C.; Rommelmann, H.; Chittipeddi, S. R.; Zhang, J. H.; Reiff, W. M.; Epstein, A. J. *J. Am. Chem. Soc.* **1987**, *109*, 769.
(2) Miller, J. S.; Epstein, A. J.; Reiff, W. M. *Science* **1988**, *240*, 40.
(3) Fontani, M.; Peters, F.; Scherer, W.; Wachter, W.; Wagner, M.; Zanello, P. *Eur. J. Inorg. Chem.* **1998**, 1453; ibid. **1998**, 2087.
(4) Lüthi, B.; Wolf, B.; Wagner, M. Unpublished results.

10.1021/om000727w CCC: $19.00
Publication on Web 11/28/2000

Scheme 1

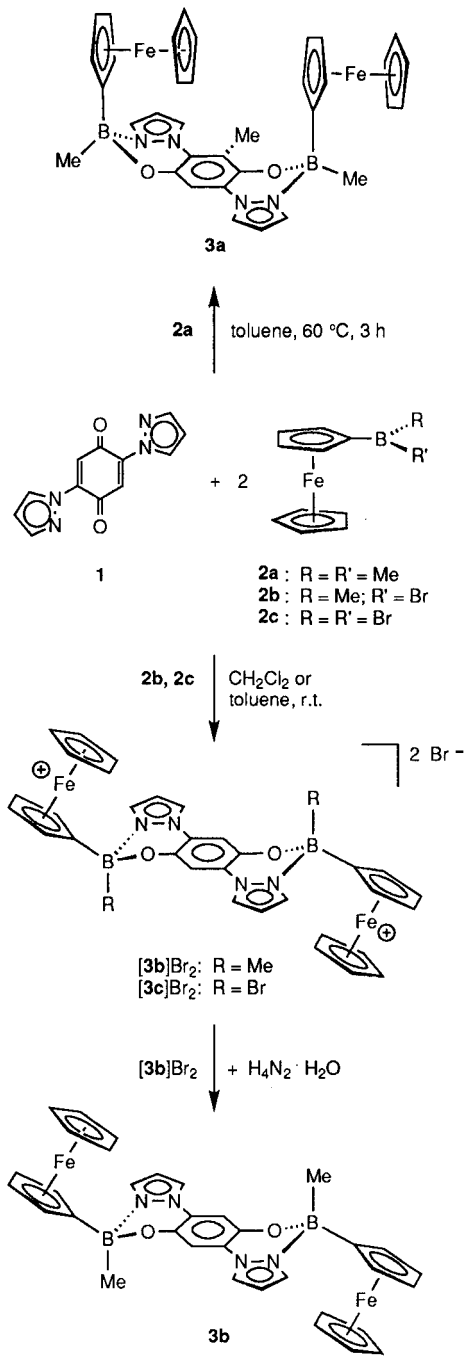

Results and Discussion

In our first attempts, ligand **1** (Scheme 1) was employed, consisting of an electron-accepting quinone unit and two pyrazole substituents, which are intended to act as anchor groups for the ferrocenylboranes. **1** is obtainable in a two-step synthesis according to literature procedures.[5] We restricted ourselves to the three derivatives **2a**−**c**[6,7] (Scheme 1) of the monoborylated ferrocene in order to generate dinuclear complexes, which are easier to characterize than polymeric target molecules **II**.

Scheme 2

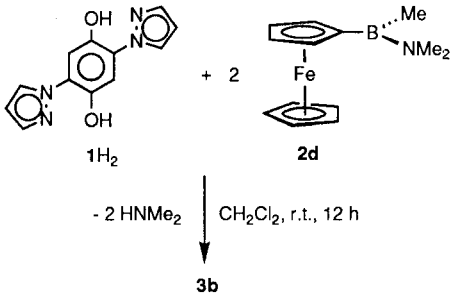

Syntheses and NMR Spectroscopy. In contrast to pyridine, **1** does not form a B−N adduct with the dimethylated ferrocenylborane **2a** at ambient temperature (toluene, ^{11}B NMR spectroscopic control). Moreover, no color change indicating a CT interaction between both components was observed. However, after heating for 3 h to 60 °C, the dinuclear complex **3a** could be isolated from the reaction mixture in 56% yield (Scheme 1). Most importantly, the two electrons required for quinone reduction are not supplied by the ferrocenyl fragments, since they still contain diamagnetic Fe(II) ions. Reduction of the quinone instead occurs by a reaction pathway which probably starts with migration of a methyl group from one boron center to the quinone ring (1,4-addition), followed by elimination of methane involving a methyl substituent of the second boron atom.

When one methyl group of **2a** is exchanged for bromide, the respective compound **2b** reacts with **1** in a different way than **2a** (Scheme 1). Upon addition of **2b** to a CH_2Cl_2 solution of **1**, the green paramagnetic precipitate [**3b**]Br_2 is formed immediately in quantitative yield. When the resulting slurry is hydrolyzed, a deep blue water phase is obtained, which is indicative of the presence of ferrocenium ions. Workup of the organic phase gave **1** in its hydroquinone state (**1**H_2, Scheme 2; approximately 30% yield), together with various byproducts resulting from incomplete hydrolysis. The experiment was thus repeated using the dibromo derivative **2c**. The reaction also generates a green paramagnetic compound ([**3c**]Br_2), which can be hydrolyzed completely under very mild conditions. Again, ferrocenium ions were detected in the water layer, but now **1**H_2 was isolated in quantitative yield after chromatography of the organic phase on a silica column. It has to be noted that with **2b** and **2c** no migration of a boron substituent to the quinone core of **1** takes place. This time, the two electrons required for quinone reduction are apparently supplied by two ferrocenes, which are in turn oxidized to their Fe(III) state. We therefore assume [**3b**]Br_2 and [**3c**]Br_2 to possess the molecular structure depicted in Scheme 1. To test this hypothesis, the more stable [**3b**]Br_2 was reduced to the diamagnetic Fe(II) state by treatment of its CH_2Cl_2 solution with a small amount of $H_4N_2 \cdot H_2O$ (Scheme 1). The compound obtained (**3b**) was identical (NMR spectroscopic control; elemental analysis) with an authentic sample synthesized by $HNMe_2$ elimination from **2d** and **1**H_2 (Scheme 2).

The ^{11}B NMR spectrum of **3a** shows a resonance at δ 4.9, which lies in a range typical of tetracoordinate boron

(5) Gauss, W.; Heitzer, H.; Petersen, S. *Liebigs Ann. Chem.* **1972**, *764*, 131.
(6) Ruf, W.; Fueller, M.; Siebert, W. *J. Organomet. Chem.* **1974**, *64*, C45.
(7) Renk, T.; Ruf, W.; Siebert, W. *J. Organomet. Chem.* **1976**, *120*, 1.

Table 1. Crystal Data and Structure Refinement Details of 1 and 3a,b

	1	3a	3b
formula	$C_{12}H_8N_4O_2$	$C_{35}H_{34}B_2Fe_2N_4O_2 \cdot 1.5CH_2Cl_2$	$C_{34}H_{32}B_2Fe_2N_4O_2 \cdot 2C_2H_6OS$
fw	240.22	803.37	818.21
cryst dimens, mm	0.40 × 0.30 × 0.10	0.40 × 0.15 × 0.05	0.40 × 0.30 × 0.10
cryst syst	monoclinic	triclinic	triclinic
space group	*C*2/*m* (No. 12)	$P\bar{1}$ (No. 2)	$P\bar{1}$ (No. 2)
temp, K	173 ± 2	173 ± 2	173 ± 2
a, Å	8.000(1)	9.017(1)	8.284(1)
b, Å	6.363(1)	14.060(2)	10.362(1)
c, Å	10.242(1)	15.639(2)	11.887(1)
α, deg	90	94.09(1)	99.40(1)
β, deg	99.08(1)	104.65(1)	97.98(1)
γ, deg	90	105.13(1)	106.12(1)
V, Å^3	514.8(1)	1831.6(4)	948.7(2)
D_c, g cm^{-3}	1.550	1.457	1.432
Z	2	2	1
radiation	Mo Kα, 0.710 73 Å	Mo Kα, 0.710 73 Å	Mo Kα, 0.710 73 Å
no. of total rflns	4943	27 652	11 673
no. of unique rflns	725	6697	3333
no. of params	56	461	254
μ, cm^{-1}	1.11	10.50	9.20
final R1[a] (all data)	0.0569	0.1165	0.0962
final wR2[b] (all data)	0.1146	0.2142	0.1774
GOF[c] (all data)	1.032	1.041	1.090

[a] $R1 = \sum(||F_o| - |F_c||)/\sum|F_o|$. [b] $wR2 = [\sum w(F_o^2 - F_c^2)^2/\sum w(F_o^2)^2]^{1/2}$. [c] $GOF = [\sum w(F_o^2 - F_c^2)^2/(NO - NV)]^{1/2}$.

nuclei.[8] The ferrocenyl fragments, the pyrazolyl rings, and the methyl groups at boron each give two equal sets of signals in the ^{1}H and ^{13}C NMR spectra, suggesting a low symmetry of the molecular framework. This conclusion is further supported by the presence of two singlets at $\delta(^1H)$ 2.66 (3H) and 7.06 (1H), indicating one of the protons at the central six-membered ring to be replaced by a methyl group. It has to be noted in this context that the integral values of the two BCH_3 resonances at 0.36 (3H) and 0.38 ppm (3H) point to a loss of one methyl group from each boron center. The resonances of the *C*O *ipso*-carbon atoms ($\delta(^{13}C)$ 142.6, 145.3) of **3a** are shifted by almost 40 ppm to higher field compared to **1** ($\delta(^{13}C)$ 182.1)[9] but possess values almost identical with those for the corresponding carbon nuclei in **1**H_2 ($\delta(^{13}C)$ 142.1).[10] It can thus be concluded that the quinone ligand **1** changed to its hydroquinone state in the course of the reaction. The integral ratios in the ^{1}H NMR spectrum of **3a** clearly reveal that the molecule consists of two ferrocenyl fragments and one bis(pyrazolyl)hydroquinone unit. The fact that both C_5H_4 rings give rise to more than two ^{1}H and ^{13}C NMR resonances suggests the boron atoms to be chiral centers.

The ^{11}B, ^{1}H, and ^{13}C NMR data of **3b** generated by reduction of [**3b**]Br_2 are exactly the same as those of a sample synthesized from **2d** and **1**H_2 (Scheme 2). In contrast to **3a**, only one set of signals is observed in the ^{1}H and ^{13}C NMR spectra of **3b**, indicating the latter molecule to possess a higher symmetry. All chemical shifts of **3b** are very similar to those of **3a** and thus do not merit further discussion.

X-ray Crystal Structure Analyses. The geometry of **1**H_2 in the solid state has been published elsewhere.[11]

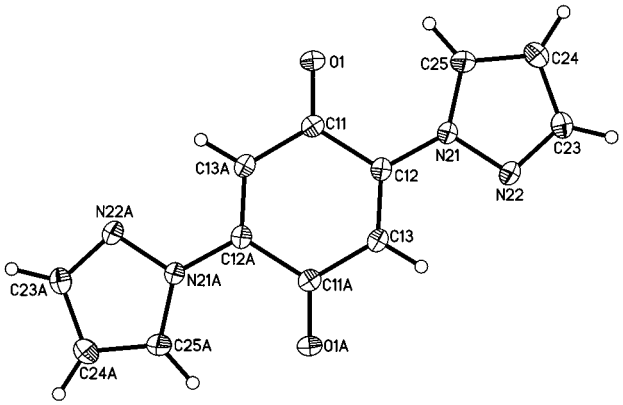

Figure 2. Molecular structure of **1**. Elements are represented by thermal ellipsoids at the 50% probability level. Selected bond lengths (Å) and torsion angles (deg): O(1)−C(11) = 1.221(2), N(21)−C(12) = 1.409(2), C(11)−C(12) = 1.508(2), C(11)−C(13A) = 1.467(2), C(12)−C(13) = 1.335(2); C(11)−C(12)−N(21)−N(22) = 180.0(0).

For comparison, we have also investigated **1** by X-ray crystallography (Table 1). The molecule possesses C_{2h} symmetry (Figure 2); all atoms are located on a crystallographic mirror plane. Perpendicular to that mirror plane, a 2-fold rotation axis passes through the center of the molecule, thereby generating a center of inversion. Bond lengths and angles of **1** show no peculiarities. **1**H_2 presents intramolecular hydrogen bonds between the OH groups of the hydroquinone fragment and the pyrazolyl nitrogen atoms N(22) and N(22A). In **1**, however, the pyrazolyl rings are turned by almost 180° about the N(21)−C(12) (N(21A)−C(12A)) axis, most likely to avoid unfavorable electrostatic interactions between the electron lone pairs of O(1) and N(22) (O(1A) and N(22A)).

Yellow X-ray-quality crystals of **3a** were grown from CH_2Cl_2 at −25 °C (Table 1; Figure 3). As has already been deduced from its NMR spectra, tetracoordinate

(8) Nöth, H.; Wrackmeyer, B. *Nuclear Magnetic Resonance Spectroscopy of Boron Compounds*; Springer: Berlin, Heidelberg, New York, 1978.

(9) Ballesteros, P.; Claramunt, R. M.; Escolástico, C.; María, M. D. S.; Elquero, J. *J. Org. Chem.* **1992**, *57*, 1873.

(10) Cornago, P.; Escolástico, C.; María, M. D. S.; Claramunt, R. M.; Carmona, D.; Esteban, M.; Oro, L. A.; Foces-Foces, C.; Llamas-Saiz, A. L.; Elguero, J. *J. Organomet. Chem.* **1994**, *467*, 293.

(11) Catalán, J.; Fabero, F.; Guijarro, M. S.; Claramunt, R. M.; Maria, M. D. S.; Foces-Foces, M. d. l. C.; Cano, F. H.; Elguero, J.; Sastre, R. *J. Am. Chem. Soc.* **1990**, *112*, 747.

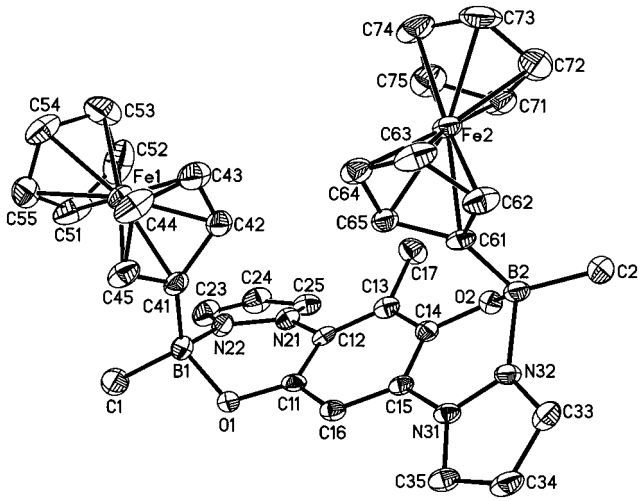

Figure 3. Molecular structure of **3a**. Elements are represented by thermal ellipsoids at the 50% probability level. Hydrogen atoms are omitted for clarity. Selected bond lengths (Å) and bond angles and torsion angles (deg): B(1)−O(1) = 1.518(8), B(2)−O(2) = 1.511(8), B(1)−N(22) = 1.618(9), B(2)−N(32) = 1.641(8), O(1)−C(11) = 1.373(7), O(2)−C(14) = 1.364(7), C(11)−C(12) = 1.410(8), C(12)−C(13) = 1.397(8), C(13)−C(14) = 1.416(8), C(14)−C(15) = 1.409(8), C(16)−C(11) = 1.380(8); C(1)−B(1)−C(41) = 116.8(5), O(1)−B(1)−N(22) = 101.3(5), C(2)−B(2)−C(61) = 116.3(5), O(2)−B(2)−N(32) = 102.0(4), O(1)−C(11)−C(12) = 120.8(5), O(1)−C(11)−C(16) = 120.4(5), O(2)−C(14)−C(13) = 119.5(5), O(2)−C(14)−C(15) = 121.5(5); C(11)−C(12)−N(21)−N(22) = 23.8(7), C(14)−C(15)−N(31)−N(32) = 16.1(7).

boron atoms bearing one methyl substituent are present in this molecule. A further methyl group is attached to the central six-membered ring which, moreover, possesses geometrical features of a hydroquinone rather than a quinone moiety: The O(1)−C(11) (O(2)−C(14)) bond length of 1.373(7) Å (1.364(7) Å) in **3a** is close to the value found for the O−C bond length in $\mathbf{1}H_2$ (1.362(3) Å)[11] but is considerably longer than the O(1)−C(11) bond of quinone **1** (1.221(2) Å). The quinone fragment in **1** shows a characteristic alternation of its C−C bond lengths (e.g. C(11)−C(12) = 1.508(2) Å; C(12)−C(13) = 1.335(2) Å). In contrast, the analogous C−C bonds in **3a** are equal within experimental error (e.g. C(11)−C(12) = 1.410(8) Å; C(12)−C(13) = 1.397(8) Å). The ferrocenyl substituents in **3a** adopt a sterically unfavorable *cis* configuration relative to the plane of the organic ligand. The entire crop of crystals, as well as their mother liquid, was investigated by NMR spectroscopy. It thus became apparent that no other isomer of **3a** had been formed in the course of the reaction.

Crystals of **3b** were grown from DMSO (Table 1). Bond lengths and angles of **3b** are very similar to those of **3a**. In contrast to **3a**, however, **3b** adopts the sterically more favored *trans* configuration (Figure 4). Again, this is true for the entire crop, as was proven by NMR spectroscopy and X-ray powder crystallography.

Electrochemical Investigations. The relevant redox potentials of **3a** and **3b**, which are compiled in Table 2, are unaffected by the different configurations of the molecules (i.e., positions of the Fc substituents *cis* or *trans* with respect to the bridging ligand).

Both compounds first undergo a single-step two-electron oxidation at about +0.2 V, which, being most likely centered on the two ferrocenes, suggests that the two Fc subunits are electronically noncommunicating. A further anodic step, having features of chemical reversibility, occurs at about +1.3 V, which in turn precedes a subsequent oxidation at about +1.6 V essentially overlapping the solvent discharge. Both steps are assigned to the oxidation of the quinoidal bridging ligand (i.e., to the sequence hydroquinone/semiquinone/quinone). Analysis[12] of the cyclic voltammograms of **3a** and **3b** with scan rates varying from 0.02 to 1.00 V s^{-1} shows that in both cases the first two-electron process displays a peak-to-peak separation ΔE_p greater than the 60 mV expected for an overall two-electron removal from two noninteracting sites. As far as the two subsequent

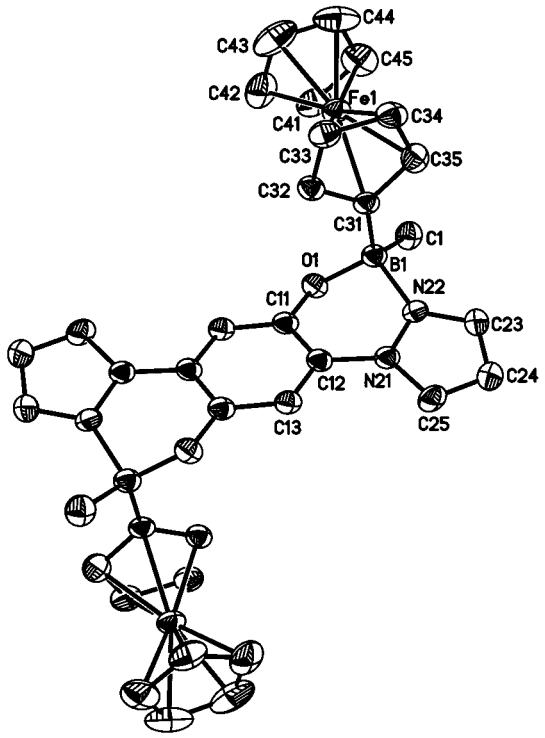

Figure 4. Molecular structure of **3b**. Elements are represented by thermal ellipsoids at the 50% probability level. Hydrogen atoms are omitted for clarity. Selected bond lengths (Å) and bond angles and torsion angles (deg): B(1)−O(1) = 1.506(7), B(1)−N(22) = 1.650(6), O(1)−C(11) = 1.369(6), C(11)−C(12) = 1.433(6), C(12)−C(13) = 1.401(7); C(1)−B(1)−C(31) = 116.2(4), O(1)−B(1)−N(22) = 103.9(4), O(1)−C(11)−C(12) = 121.6(4), O(1)−C(11)−C(13*) = 120.6(4); C(11)−C(12)−N(21)−N(22) = 13.3(6). The asterisk denotes a symmetry transformation used to generate equivalent atoms: $-x + 2$, $-y + 2$, $-z + 2$.

Table 2. Formal Electrode Potentials (in V, vs SCE) and Peak-to-Peak Separations (in mV) for the Oxidation Processes of 3a,b in Dichloromethane Solution

	Fc-centered process		ligand-centered processes		
	$E^{\circ\prime}$	ΔE_p [a]	$E^{\circ\prime}$	ΔE_p [a]	E_p [a,b]
3a	+0.20[c]	88	+1.26	78	+1.6
3b	+0.18[c]	72	+1.27	64	+1.6
FcH	+0.39[d]	78			

[a] Measured at 0.2 V s^{-1}. [b] Peak potential of the irreversible process. [c] Two-electron oxidation. [d] One-electron oxidation.

(12) Brown, E. R.; Sandifer, J. In *Physical Methods in Chemistry: Electrochemical Methods*; Rossiter, B. W., Hamilton, J. F., Eds.; Wiley: New York, 1986.

oxidation processes are concerned, only the first one exhibits features of electrochemical quasireversibility. This step, however, also appears to be coupled to chemical complications, since the $i_{p,c}/i_{p,a}$ value is lower than unity at low scan rates. Exhaustive oxidation at $E_w = 0.8$ V, which confirms the two-electron nature of the first anodic process, causes the yellow solutions of **3a** and **3b** to turn green-blue. At the same time, the poor solubility of **3b** in CH_2Cl_2 is considerably improved. In the UV−vis spectra of **3a** and **3b**, an absorption at $\lambda = 620$ nm, with a shoulder at 530 nm, develops and increases in intensity while the oxidation is carried on. The cyclic voltammetric profiles of $\mathbf{3a}^{2+}$ and $\mathbf{3b}^{2+}$ are complementary to those of the neutral species, thereby confirming the full chemical reversibility of the Fc oxidations.

Conclusion

Given our previous findings[3] that base adducts of ferrocenylboranes possess a significantly lower redox potential than the parent Lewis acids, the results presented in this paper may be interpreted in the following way: The reaction of $FcBMe_2$ (**2a**) with bis(pyrazol-1-yl)benzoquinone (**1**) does not give a B−N adduct. Consequently, no electron transfer from iron to the benzoquinone acceptor takes place. In contrast, the more Lewis acidic derivatives FcB(Me)Br (**2b**) and $FcBBr_2$ (**2c**) are likely to form B−N adducts with **1** in the initial reaction step, which promotes oxidation of the electron-rich ferrocene donor by the electron-poor benzoquinone moiety and leads to the paramagnetic ferrocenium compounds [**3b**]Br_2 and [**3c**]Br_2. On the basis of the high-yield synthesis of **3b** (Scheme 2), work is currently in progress to generate poly(ferrocenylene) macromolecules from $\mathbf{1}H_2$ and the diborylated ferrocene 1,1′-fc[B(Me)NMe_2]$_2$ (fc = $(C_5H_4)_2Fe$). Subsequent oxidation of the iron centers (and hydroquinone bridges) should lead to paramagnetic spin chains.

The initial target structure **II** (Figure 1) is probably not obtainable using the quinone acceptor **1**, because B−O bond formation cannot be prevented after the charge transfer has taken place. Therefore, e.g. a tetracyanoquinone rather than a benzoquinone-based ligand has to be employed as electron acceptor.

Experimental Section

General Considerations. All reactions and manipulations of air-sensitive compounds were carried out in dry, oxygen-free argon using standard Schlenk ware. Solvents were freshly distilled under N_2 from Na/K alloy−benzophenone (toluene, hexane) or from CaH_2 (CH_2Cl_2) prior to use; DMSO was dried using molecular sieves (4 Å). NMR: Bruker AMX 250, Bruker DPX 250, Bruker AMX 400 spectrometers. Abbreviations: s = singlet; d = doublet; tr = triplet; vtr = virtual triplet; nr = multiplet expected in the ^{1}H NMR spectrum, but not resolved; pz = pyrazolyl; hqui = hydroquinone. ^{11}B NMR spectra are reported relative to external $BF_2{\cdot}Et_2O$. Elemental analyses: Microanalytical laboratory of the J. W. Goethe-Universität Frankfurt.

Synthesis of 3a. A toluene (10 mL) solution of **2a** (0.27 g, 1.20 mmol) was added with stirring at room temperature to a suspension of **1** (0.14 g, 0.58 mmol) in 25 mL of toluene. The mixture was stirred at 60 °C for 3 h, and a clear orange solution formed, which was then cooled to room temperature. Upon addition of hexane (40 mL), a yellow microcrystalline solid precipitated, which was isolated by filtration and dried in vacuo. Yield: 0.22 g (56%). Orange X-ray-quality crystals of **3a** were grown from CH_2Cl_2 at −25 °C.

^{11}B NMR (128.3 MHz, $CDCl_3$): δ 4.9 ($h_{1/2}$ = 380 Hz). ^{1}H NMR (250 MHz, $CDCl_3$): δ 0.36, 0.38 (2 × s, 2 × 3H; BCH_3), 2.66 (s, 3H; hqui-CH_3), 3.83, 3.87, 3.99, 4.07, 4.09, 4.12 (6 × nr, 2H, 1H, 1H, 3H, 5H, 6H; C_5H_4, C_5H_5), 6.58, 6.65 (2 × vtr, ^3J(H,H) = 2.6 Hz, 2 × 1H; pz-H4), 7.06 (s, 1H; hqui-H), 7.61, 7.72, 7.96, 8.10 (4 × d, ^3J(H,H) = 2.6 Hz, 4 × 1H; pz-H3,5). ^{13}C NMR (100.5 MHz, $CDCl_3$): δ 6.2 (BCH_3), 14.2 (hqui-CH_3), 68.5 (C_5H_5), 69.1, 69.2, 69.3, 71.1, 72.3, 72.8 (C_5H_4), 105.6, 107.5, 108.3 (hqui-*C*H, pz-C4), 119.5, 124.1, 126.4 (hqui-*C*CH_3, hqui-CN), 127.0, 131.0, 133.9, 134.0 (pz-C3,5), 142.6, 145.3 (hqui-CO); C_5H_4-*ipso* not observed. Anal. Calcd for $C_{35}H_{34}B_2Fe_2N_4O_2$ (675.99): C, 62.19; H, 5.07; N, 8.29. Found: C, 61.97; H, 5.25; N, 8.00.

Synthesis of [3b]Br_2. A CH_2Cl_2 (80 mL) solution of **1** (0.30 g, 1.25 mmol) was added with stirring at room temperature to a solution of **2b** (0.78 g, 2.68 mmol) in 20 mL of CH_2Cl_2. The mixture instantaneously adopted a green color with the formation of a green precipitate. The slurry was stirred overnight, and all insolubles were isolated by filtration, washed with hexane (2 × 20 mL), and dried in vacuo. Yield: 0.81 g (79%). Anal. Calcd for $C_{34}H_{32}B_2Br_2Fe_2N_4O_2$ (821.77): C, 49.69; H, 3.92; N, 6.82. Found: C, 49.49; H, 4.01; N, 6.66.

Synthesis of 3b. Method 1. To a green suspension of [**3b**]Br_2 (0.13 g, 0.16 mmol) in CH_2Cl_2 (10 mL) were added three drops of hydrazine monohydrate. The mixture changed color from deep green to yellow. The mother liquid was removed using a filter cannula, and the solid residue was triturated with hexane (2 × 20 mL) and dried in vacuo. Yield: 0.08 g (76%).

Method 2. A CH_2Cl_2 (20 mL) solution of $\mathbf{1}H_2$ (0.14 g, 0.57 mmol) was added with stirring at room temperature to a solution of **2d** (0.29 g, 1.14 mmol) in 10 mL of CH_2Cl_2. A yellow precipitate formed slowly within several hours, and the mixture was stirred overnight. The mother liquid was removed using a filter cannula, and the solid residue was triturated with hexane (2 × 20 mL) and dried in vacuo. Yield: 0.36 g (95%). Orange X-ray-quality crystals were grown by recrystallization of **3b** from DMSO.

^{11}B NMR (128.3 MHz, [D_6]DMSO, 80 °C): δ 1.7 ($h_{1/2}$ = 300 Hz). ^{1}H NMR (250 MHz, [D_6]DMSO, 80 °C): δ 0.34 (s, 6H; BCH_3), 3.77 (nr, 4H; C_5H_4), 3.95 (s, 10H; C_5H_5), 3.97 (nr, 4H; C_5H_4), 6.87 (nr, 2H; pz-H4), 7.58 (s, 2H; hqui-H), 8.08, 8.91 (2 × nr, 2 × 2H; pz-H3,5). ^{13}C NMR (100.5 MHz, [D_6]DMSO, 80 °C): δ 67.0 (C_5H_5), 67.4, 70.4 (C_5H_4), 107.3, 107.9 (hqui-*C*H, pz-C4), 123.5 (hqui-CN), 128.5, 134.3 (pz-C3,5), 141.8 (hqui-CO); BCH_3 and C_5H_4-*ipso* not observed. Anal. Calcd for $C_{34}H_{32}B_2Fe_2N_4O_2$ (661.97) + 0.25 CH_2Cl_2 (84.93): C, 60.21; H, 4.79; N, 8.20. Found: C, 60.15; H, 4.86; N, 8.06.

Synthesis of [3c]Br_2. A toluene (10 mL) solution of **2c** (0.35 g, 0.98 mmol) was added dropwise with stirring at room temperature to a solution of **1** (0.12 g, 0.49 mmol) in 40 mL of toluene. The mixture instantaneously adopted a green color with the formation of a green precipitate. The slurry was stirred overnight, and all insolubles were isolated by filtration, washed with hexane (2 × 20 mL), and dried in vacuo. Yield: 0.39 g (84%). Anal. Calcd for $C_{32}H_{26}B_2Br_4Fe_2N_4O_2$ (951.51): C, 40.39; H, 2.75; N, 5.89. Found: C, 40.01; H, 2.42; N, 5.85.

Hydrolysis of [3c]Br_2. H_2O (20 mL) was added to solid [**3c**]Br_2 (0.16 g, 0.17 mmol) and the resulting slurry stirred for 10 min. A gray insoluble material precipitated from the deep blue water phase. The solid was dissolved in $CHCl_3$ and purified by chromatography (silica gel) to give pure $\mathbf{1}H_2$. Yield: 0.04 g (97%).

Crystal Data for 1. An orange platelet of **1** was mounted on top of a glass filament on a CCD diffraction system (Bruker AXS). Final lattice parameters were obtained by least-squares refinement of 2334 reflections. Data were collected at 173(2) K, with a crystal-to-detector distance of 40 mm (2.01° < θ <

28.69°). Data were corrected for Lorentz and polarization terms; an empirical absorption correction was applied.[13] The structure was solved by direct methods[14] (R(int) = 0.0605) and refined against F^2 with full-matrix least-squares methods.[15] All hydrogen atoms were found and refined using a riding model. A total of 56 parameters were refined: 13.0 data per parameter, $w = 1/[\sigma^2(F_o^2) + (0.0732P)^2]$ where $P = (F_o^2 + 2F_c^2)/3$, shift/error < 0.0001 in the last cycle of refinement, residual electron density +0.477 and −0.218 e Å^{-3}, minimized function $\sum w((F_o^2) - (F_c^2))^2$.

Crystal Data for 3a. A yellow crystal of **3a**·1.5CH_2Cl_2 was mounted on top of a glass filament on a CCD diffraction system (Bruker AXS). Final lattice parameters were obtained by least-squares refinement of 7092 reflections. Data were collected at 173(2) K, with a crystal-to-detector distance of 40 mm (1.88° < θ < 25.35°). Data were corrected for Lorentz and polarization terms; an empirical absorption correction was applied.[13] The structure was solved by direct methods[14] (R(int) = 0.0826) and refined against F^2 with full-matrix least-squares methods.[15] Hydrogen atoms were calculated in ideal positions (riding model); disordered CH_2Cl_2 was refined in two positions. A total of 461 parameters were refined: 14.5 data per parameter, $w = 1/[\sigma^2(F_o^2) + (0.1124P)^2 + 5.1395P]$ where $P = (F_o^2 + 2F_c^2)/3$, shift/error < 0.0001 in the last cycle of refinement, residual electron density +2.510 and −1.065 e Å^{-3}, minimized function $\sum w((F_o^2) - (F_c^2))^2$.

Crystal Data for 3b. A yellow crystal of **3b**·2DMSO was mounted on top of a glass filament on a CCD diffraction system (Bruker AXS). Final lattice parameters were obtained by least-squares refinement of 6457 reflections. Data were collected at 173(2) K, with a crystal-to-detector distance of 51 mm (1.77° < θ < 25.03°). Data were corrected for Lorentz and polarization terms; an empirical absorption correction was applied.[13] The structure was solved by direct methods[14] (R(int) = 0.0671) and refined against F^2 with full-matrix least-squares methods.[15] Hydrogen atoms were calculated in ideal positions (riding model); disordered DMSO was refined in two positions. A total of 254 parameters were refined: 13.1 data per parameter, $w = 1/[\sigma^2(F_o^2) + (0.0873P)^2 + 1.4261P]$ where $P = (F_o^2 + 2F_c^2)/3$, shift/error < 0.0001 in the last cycle of refinement, residual electron density +0.520 and −0.888 e Å^{-3}, minimized function $\sum w((F_o^2) - (F_c^2))^2$.

Acknowledgment. Financial funding by the "Deutsche Forschungsgemeinschaft" (DFG) and the "Fonds der Chemischen Industrie" (FCI) is acknowledged. L.D. is grateful to the "Alexander von Humboldt Foundation" for a postdoctoral grant.

Supporting Information Available: Figures giving packing diagrams and crystallographic files, in CIF format, for **1** and **3a**,**b**. This material is available free of charge via the Internet at http://pubs.acs.org.

OM000727W

(13) Sheldrick, G. M. *SADABS: A Program for Empirical Absorption Correction of Area Detector Data*; Universität Göttingen, Göttingen, Germany, 1996.

(14) Sheldrick, G. M. *Acta Crystallogr.* **1990**, *A46*, 467.

(15) Sheldrick, G. M. *SHELXL-97: A Program for the Refinement of Crystal Structures*; Universität Göttingen, Göttingen, Germany, 1997.